

Automatic Detection of Fetal Nasal Bone in 2 Dimensional Ultrasound Image Using Map Matching

LAI KHIN WEE, EKO SUPRIYANTO

Department of Clinical Science and Engineering

Universiti Teknologi Malaysia

UTM Skudai, 81310 Johor

MALAYSIA

laikw2@gmail.com eko@utm.my <http://www.biomedical.utm.my>

Abstract: - Recent study shows that fetal chromosomal abnormalities can be detected in early ultrasonic prenatal screening by identifying the absence of fetus nasal bone. The drawbacks of current method are operator dependent, observer variability and its inefficiency. In particular, accurate nasal bone detection requires highly trained sonographers and obstetrics and gynecology specialists since the ultrasound markers may easily confuse with noise and echogenic line in ultrasound image background. We present a computerized method of detecting the absent of nasal bone by using map matching computerized method. Image preprocessing is implemented prior map matching based on image correlation to assess the availability of nasal bone. The resultant threshold bordering the absent and present of nasal bone is set to value 0.35. The threshold can be further improved if a larger set of nasal bone ultrasound images applied.

Key-Words: - Chromosomal abnormalities, nasal bone, mapping matching, ultrasound image

1 Introduction

The presence of fetal chromosomal abnormalities such as trisomy 21 can be recognized through premature ultrasound prenatal screening. Recent studies shows that assessment of particular ultrasound markers offer promising invasive method for fetal abnormalities detection, such as nuchal translucency, nasal bone, long bone biometry and ductus venous [1]. Based on previous literatures, it shows that noses of babies with trisomy may have a small or poorly formed nasal bone structure which usually does not show up during the scan in early pregnancy [2]. Therefore, assessment of fetal nasal bone improves the performance of first trimester screening for trisomy 21 [3]. R. Has et al. [4] had reported that the absence of fetal nasal bone has a high positive likelihood ratio for Down syndrome in the first trimester screening, and the presence of nasal bone may potentially lower the need for invasive testing. Same researches has been conducted on fetal from 15 to 24 weeks gestation old also reported that nasal bone hypoplasia is associated with an increased risk of Down syndrome in the presented population [5]. F. Orlandi et al. [6] concluded that absence of the nasal bone can be used as a marker for abnormalities screening and they have demonstrated inclusion of nasal bone in current screening protocol along with nuchal translucency, free beta-hCG and PAPP-A can achieve high detection at a very low false-positive rate. Normally, the nasal bone is evaluated in the sagittal section of fetus by transabdominal or transvaginal ultrasound examination.

While ultrasonography probe was position on neutral point of fetus, three hyperechogenic lines parallel to nasal bone were observed. It was especially paid attention not to mistake nasal bone with echogenic skin line of nose. The ultrasonographic sagittal view of a fetus with nasal bone is shown in Fig. 1.

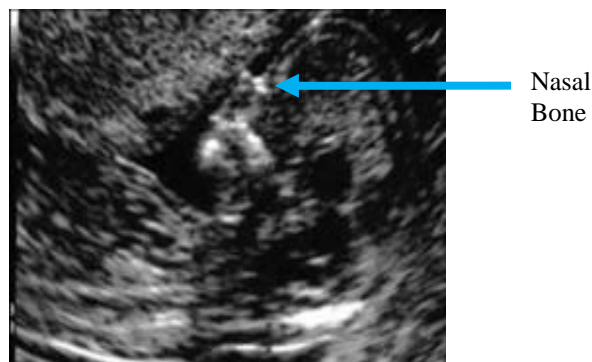


Fig. 1 Ultrasonographic sagittal view of fetus with nasal bone

M. Chen et al. [7] had investigated the measurement of nasal bone by using 3D volume ultrasound fetal data during early pregnancy. Acquisition of three dimensional volumes data were record in mid-sagittal plane and examined using multiplanar techniques but result shows that 3D measurement offers no advantages over 2D sonography. Among the other previous work done on automatic fetal measurements, researches topics are more focusing on automatic nuchal translucency

thickness measurement, and of automatic detection of nasal bone have not been addressed by many authors.

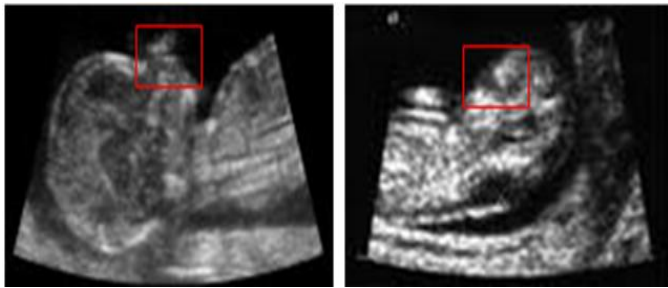


Fig. 2 Different location of nasal bone due to different position of fetus in 2 dimensional ultrasound images

In this paper, we presented an automatic method to recognize and detect the fetal nasal bone based on 2 dimensional ultrasound images using map matching techniques. Prior to assess the absent of nasal bone, several image preprocessing techniques were implemented to trace the position of nasal bone due to random shape and position of embryo in ultrasound images. Fig. 2 illustrates different location of nasal bone due to different position of fetus in ultrasound images and Fig. 3 displays each important step toward abnormalities detection.

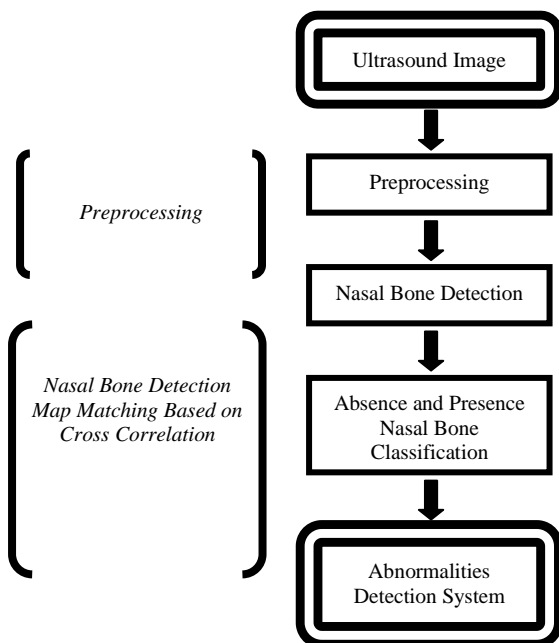


Fig. 3 Sequences of algorithm for each important processing

The rest of this paper is organized as follows. In section 2, we describe the procedure of image acquisition, the characteristics of the nasal bone images and the

detection procedure of the nasal bone. The results of present method are shown in Section 3, and finally we draw some conclusions in Section 4.

2 Material and Methods

In this section, we describe the procedure of image acquisition, the characteristics of the nasal bone images and explain the recognition and detection procedure. The images of fetal with nasal bone were acquired using KNOTRON (Sigma 330 Expert) ultrasound machine with a 3.5MHz convex transducer. A mid-sagittal view of the fetal profile is obtained with the ultrasound transducer being held parallel to the longitudinal axis of the nasal bone. The angle of insonation is crucial because the nasal bone will not be visible almost invariably when the longitudinal axis of the bone is perpendicular to the ultrasound transducer. In the correct view, there are 3 distinct lines. The first 2 lines, which are proximal to the forehead, are horizontal and parallel to each other, resembling an “equal sign.” The top line represents the skin and the bottom line, which is thicker and more echogenic than the overlying skin, represents the nasal bone. A third line, which is almost in continuity with the skin but at a higher level, represents the tip of the nose [8]. They were saved into processing unit through our unique developed hardware in DICOM format. Fig. 4 below shows the block diagram of image acquisition from ultrasound machine to our developed hardware.

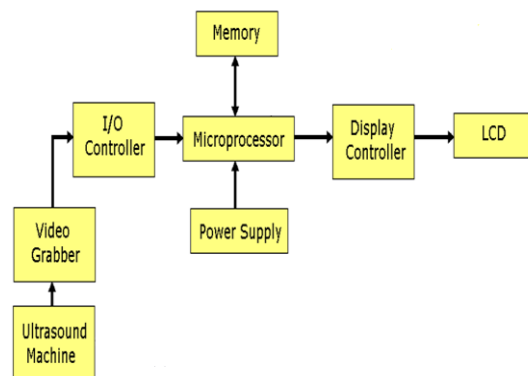


Fig. 4 Block diagram of image acquisition from ultrasound machine

2.1 Characteristics of nasal bone images

Ossifications in nasal bones are being delayed in fetuses with trisomy. Current studies, maintains that Down syndrome and other chromosome anomalies should be scanned in the first trimester of gestation and various studies are done for that reason. Nasal bone evaluation in 11-13+6 weeks is quite hard even for experienced people. Nasal bone is a structure which actually formed of two separate bones and only seen by ultrasonography

after 10th gestational week. If it is not examined in an appropriate plan, it may be measured shorter or longer than normal or even it may be supposed that it does not exist.

2.2 Map matching

Map image matching has been a subject of research as early as the 80’s. Since then, researchers have proposed several methods, battling against numerous demands from industries. The main difficulty in the present method is maintaining tolerance against various image distortions that can occur during image input. Such distortions include, but are not limited to, rotation, changes in size, linear and non-linear changes in brightness, perspective distortion, and noise. Aside from accuracy and precision, efficiency is also an important element in constructing the full algorithm [9].

As industries involving the handling of small parts increase, intelligent vision robots are being demanded to replace human inspectors. As opposed to human inspectors, artificial intelligence provides tolerance to long work hours and high repeatability. Consequently, there have been extensive studies in computer vision, especially in the field of map image matching. However, no effective algorithm that can match the human eye and brain has yet been discovered [9]. The algorithm introduced in present method can be regarded as an “upgrade” to what has already been discovered. It attempts to ease several difficulties that were present in previous matching algorithms.

2.3 Architecture of map matching with normalized grayscale correlation algorithm

Let’s assume a given image S with matrix size $P \times Q$ and image T with matrix size $M \times N$, where the dimensions of S are both larger than T . We proposed to call T as the Template Image $T_{i,j}$, and call the pattern in T as the Template Pattern, as well as calling S as the Search Image, $S_{i,j}$ as shown below,

$$\bar{S}_{i,j} = \frac{1}{m \times n} \sum_{i=0, j=0}^{n-1, m-1} S_{i+x, j+y} \tag{1}$$

$$\bar{T} = \frac{1}{m \times n} \sum_{i=0, j=0}^{n-1, m-1} T_{i,j} \tag{2}$$

Then, the output of S contains a subset image I where I and T are suitably similar in pattern and if such I exists; yield the location of I in S . The location of I in S will be referred to as the location of closest match, which will then been defined as the pixel index of the top-left corner of I in S .

$$\lambda(i,j) = \frac{\mathfrak{z}(S_{i+x+y} - \bar{S}_{i,j}) \mathfrak{z}(T_{x,y} - \bar{T})}{\sqrt{\mathfrak{z}(S_{i+x+y} - \bar{S}_{i,j})^2 \mathfrak{z}(T_{x,y} - \bar{T})^2}} \tag{3}$$

Where $\mathfrak{z} = \sum_{x=0, y=0}^{n-1, m-1}$ and $0 \leq i \leq p-n, 0 \leq j \leq q-m$

Let $\lambda(i,j)$ be the correlation coefficient of T at location i,j of S , as defined in equation 3. The maximum value of λ is set to value 1. Therefore, whenever the coordinate integers of (i,j) be such that $\lambda(i,j)$ obtained the highest correlation coefficient. The algorithm will return i,j as the “closest match” in S .

2.4 Image correlation

The normalized cross-correlation is calculated using equation 4 and will be displayed as a surface plot. The peak of the cross-correlation matrix occurs where the template image and target image are best correlated. However, algorithm must convert the image into grayscale before calculation of image correlation.

Equation 4 computes the normalized cross-correlation of the matrices template and target. The target matrix must be larger than the template matrix in order to make the normalization meaningful. Nevertheless, the values of template cannot all be the same. The resulting matrix contains the correlation coefficients, which can range in value from -1.0 to 1.0.

$$\gamma(u,v) = \frac{\sum_{x,y} [f_{x,y} - \bar{f}_{u,v}] [t_{x-u, y-v} - \bar{t}]}{\sum_{x,y} [f_{x,y} - \bar{f}_{u,v}]^2 \sum_{x,y} [t_{x-u, y-v} - \bar{t}]^2} \tag{4}$$

Where f = image, t = mean of template and $f_{u,v}$ is the mean of $f(x,y)$ in the region under the template. After calculated the image correlation, the next step of the developed algorithm is to convert the image correlation into surface plotting graph as shown in Fig. 5. Based on the graph, we are able to obtain the maximum value of the image correlation which will be used for image classification of absence and presence nasal bone eventually.

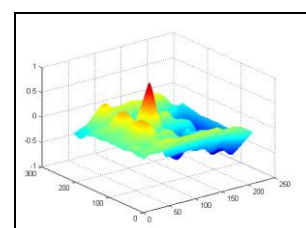


Fig. 5 Experimental sample result of image correlation

3 Result and Analysis

In order to justify the performance of developed computerized algorithm, two different groups of testing images $k1$, $k2$ were used. The group $k1$ were randomly selected images with nasal bone screening from a consecutive group of registered patients by using the same ultrasound scanner as the one used in training, and the second group of images $k2$ are the images with no nasal bone found collected from Health Centre, Universiti Teknologi Malaysia. The first group of testing catalogue consisting 30 numbers of ultrasound fetal images, where the second catalogue only contains 7 ultrasound images because of the limitation of sources. After all the images cross correlation been calculated, the result are analyzed and the classified simulation shows that the peak of plot graph will always below than the value 0.35 whenever an ultrasound images without nasal bone was tested. Fig. 6 below shows the comparison of absent and present of nasal bone.

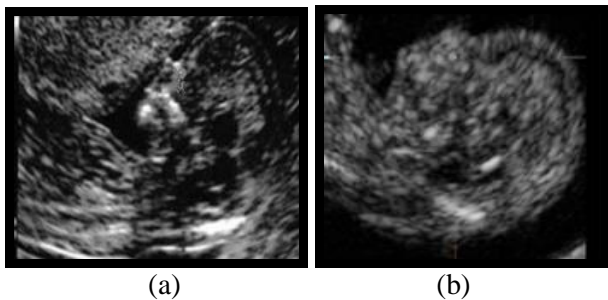
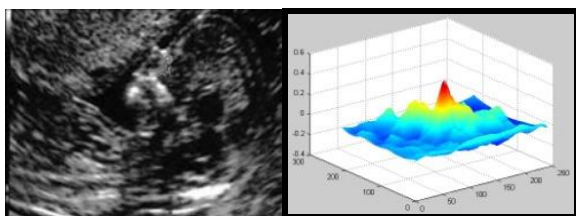
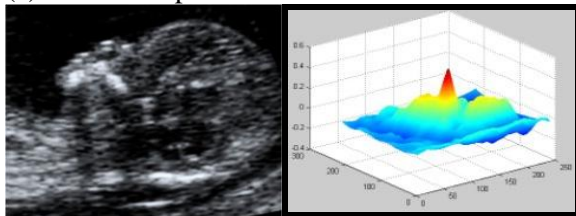


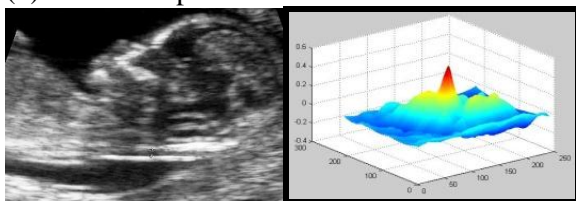
Fig. 6 shows the comparison of ultrasound sample images (a) with nasal bone (b) without nasal bone



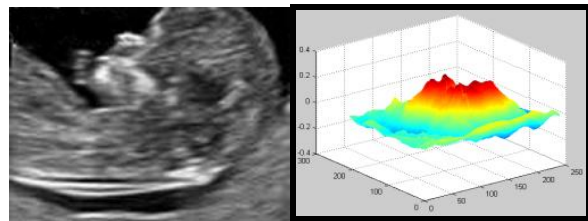
(a) Maximum peak value 0.5701



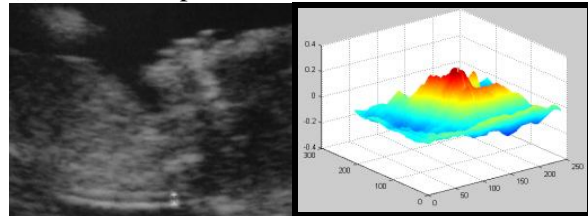
(b) Maximum peak value 0.4578



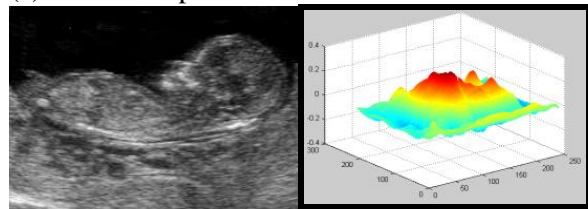
(c) Maximum peak value 0.5700



(d) Maximum peak value 0.2714



(e) Maximum peak value 0.3331



(f) Maximum peak value 0.3085

Fig. 7 shows part of the experimental results for images group $k1$ (a), (b) and (c), and images group $k2$ (d), (e), (f).

Base on the results from the experimental simulations, the developed algorithm will classify the threshold as value 0.35 when the images were found absent of nasal bone. However, the limitation of the software is to acquire the correct scanning plane of two dimensional ultrasound fetal images. If the tested images are not in the true sagittal view or coincide in the suitable plane, ultrasound markers might not appears in appropriate position. To encounter the limitation mentioned above, we are under investigation of real time techniques to select the optimum plane of two dimensional ultrasound images in an automatic way during the scanning procedure.

4 Conclusion

We have proposed a method for automatic nasal bone recognition and detection based on map matching techniques. From this method we are able to classify the absence and presence of nasal bone based on the obtained parameter value from the image correlation graph. The threshold bordering the absent and present of nasal bone is set to value 0.35. The threshold can be further improved if a larger set of nasal bone ultrasound images applied. Findings showed that the system is able to provide consistent and reproducible results.

ACKNOWLEDGMENTS

The authors would like to express our thankfulness to Health Centre, Universiti Teknologi Malaysia and Ministry of Science, Technology and Innovation (MOSTI), Malaysia for supporting and funding part of this study under Vote 79327. Our appreciation also goes to the Progressive Healthcare and Human Development Research Group members for their ideas and comments on this paper.

References:

- [1] Nicolaides, K., Sebire, N., Snijders, R., "The 11-14 weeks scan: the diagnosis of fetal abnormalities", Parthenon Publishing, NY, 1999.
- [2] C. Larose, P. Massoc, Y. Hillion, J.P. Bernard, Y. Ville, "Comparison of fetal nasal bone assessment by ultrasound at 11-14 weeks and by postmortem X-ray in trisomy 21: a prospective observational study", *Ultrasound in Obstetrics and Gynecology*, John Wiley & Sons, Ltd, Volume 22, Pages 27-30, 2003.
- [3] K.O. kagan, S. Cicero, I. Staboulidou, D. Wright, K.H. Nicolaides, "Fetal nasal bone in screening for trisomies 21, 18 and 13 and turner syndrome at 11-13 weeks of gestation", *Ultrasound in Obstetrics and Gynecology*, John Wiley & Sons, Ltd, Volume 33, Pages 259-264, 2004.
- [4] Recep Has, Ibrahim Kalelioglu, Atil Yuksel, Lemi Ibrahimoglu, Hayri Ermis, Alkan Yildirim, "Fetal Nasal Bone Assessment in First Trimester Down Syndrome Screening", *Fetal Diagn Ther*, Volume 24, pages 61-66, 2008.
- [5] B. Naraphut, B. Uerpairojkit, S. Chaithongwatthana, Y. Tannirandorn, S. Tanawattanacharoen, S. Manotaya, D. Charoenvidhya, "Nasal Bone Hypoplasia in Trisomy 21 at 15 to 24 Weeks' Gestation in A High Risk Thai Population", *J Med Assoc Thai*, Volume 89(7), pages 911-917, 2006.
- [6] F. Orlandi, C.M. Bilardo, M. Campogrande, D. Krantz, T. Hallahan, C. Rossi, E. Viora, "Measurement of nasal bone length at 11-14 weeks of pregnancy and its potential role in Down syndrome risk assessment", *Ultrasound Obstet Gynecol*, Wiley InterScience, DOI: 10.1002/uog.167.
- [7] M. Chen, H.F. Wang, T.Y. Leung, T.Y. Fung, L.W. Chan, D.S. Sahota, T.H.T. Lao, T.K. Lau, "First Trimester Measurement of Nasal Bone Length Using Three Dimensional UltraSound", *Prenatal Diagnosis*, John Wiley & Sons, Ltd, Volume 29, Pages 766-770, 2009.
- [8] Kypros H. Nicolaides, "Nuchal translucency and other first-trimester sonographic markers of chromosomal abnormalities", *American Journal of Obstetrics and Gynecology*, Volume 191, pages 45-67, 2004.
- [9] Ryo Takei, "A New Grey-Scale Template Image Matching Algorithm Using The Cross-Sectional Histogram Correlation Method", July 2003.